Xist imprinting is promoted by the hemizygous (unpaired) state in the male germ line

Sha Sun[a,b,c], Bernhard Payer[a,b,1], Satoshi Namekawa[d,e], Jee Young An[a,b,2], William Press[a,b], Jovani Catalan-Dibene[c], Hongjae Sunwoo[a,b], and Jeannie T. Lee[a,b,f,3]

[a]Department of Molecular Biology, Massachusetts General Hospital, Harvard Medical School, Boston, MA 02114; [b]Department of Genetics, Harvard Medical School, Boston, MA 02114; [c]Department of Developmental and Cell Biology, School of Biological Sciences, University of California, Irvine, CA 92697; [d]Division of Reproductive Sciences, Perinatal Institute, Cincinnati Children's Hospital Medical Center, Cincinnati, OH 45229; [e]Department of Pediatrics, University of Cincinnati College of Medicine, Cincinnati, OH 45229; and [f]Howard Hughes Medical Institute, Harvard Medical School, Boston, MA 02114

This contribution is part of the special series of Inaugural Articles by members of the National Academy of Sciences elected in 2015. Contributed by Jeannie T. Lee, October 1, 2015 (sent for review July 29, 2015; reviewed by Nora Engel and Kathrin Plath)

The long noncoding X-inactivation–specific transcript (*Xist* gene) is responsible for mammalian X-chromosome dosage compensation between the sexes, the process by which one of the two X chromosomes is inactivated in the female soma. *Xist* is essential for both the random and imprinted forms of X-chromosome inactivation. In the imprinted form, *Xist* is paternally marked to be expressed in female embryos. To investigate the mechanism of *Xist* imprinting, we introduce *Xist* transgenes (Tg) into the male germ line. Although ectopic high-level *Xist* expression on autosomes can be compatible with viability, transgenic animals demonstrate reduced fitness, subfertility, defective meiotic pairing, and other germ-cell abnormalities. In the progeny, paternal-specific expression is recapitulated by the 200-kb *Xist* Tg. However, *Xist* imprinting occurs efficiently only when it is in an unpaired or unpartnered state during male meiosis. When transmitted from a hemizygous father (+/Tg), the *Xist* Tg demonstrates paternal-specific expression in the early embryo. When transmitted by a homozygous father (Tg/Tg), the Tg fails to show imprinted expression. Thus, *Xist* imprinting is directed by sequences within a 200-kb X-linked region, and the hemizygous (unpaired) state of the *Xist* region promotes its imprinting in the male germ line.

Xist | imprinting | X inactivation | transgenerational inheritance | meiotic silencing by unpaired DNA

In mammals, the balance of X-linked gene dosage between XX females and XY males is achieved through X-chromosome inactivation (XCI) (1–4). Although marsupial mammals exhibit imprinted XCI and thereby inactivate only the paternally derived X chromosome (X^P), placental mammals demonstrate two forms of XCI: Imprinted X^P inactivation in the early embryo and trophectoderm and random X inactivation in embryonic (epiblast) tissues (5–7). In placental mammals, both imprinted and random XCI are controlled by the X-inactivation center (*Xic*), which is located on the X chromosome and is necessary and sufficient to direct the silencing for an entire X chromosome in the female mammal (8, 9). As a master regulatory locus, the *Xic* contains multiple long noncoding RNAs (lncRNAs) including Xist X-inactivation–specific transcript (Xist), a 17-kb noncoding transcript which coats the inactive X chromosome (Xi) and initiates silencing (3, 10).

Xist is required for both random XCI and imprinted X^P inactivation (11–14). During random XCI, *Xist* is up-regulated exclusively from the future Xi at the same time that expression of its antisense partner, Tsix (15), is down-regulated *in cis*. During imprinted XCI, *Xist* is expressed for the first time from the X^P at the time of zygotic gene activation in the two-cell embryo (16, 17). In the paternal germ line, however, Xist RNA is expressed only at low levels, suggesting that it is not required for spermatogenesis (18, 19). Consistent with this notion, male mice with an *Xist* deletion are fertile (12, 20).

Although significant progress has been made in understanding the control of *Xist* expression for random XCI, the control of imprinted XCI is still poorly understood (2, 4, 16, 21–23). Work with parthenogenetic embryos has provided evidence for both a maternal and a paternal imprint (24–27). For example, X^MX^M gynogenetic embryos bearing two maternal genomes and (therefore two maternal X chromosomes [X^M]) block *Xist* expression despite possessing two X chromosomes, thereby arguing that the oocyte imprints the *Xist* gene to resist expression from the X^M in the early embryo. On the other hand, X^PX^P androgenetic embryos bearing two paternal genomes and (therefore two X^P) display two foci of *Xist* expression, indicating that the male germ line imprints the *Xist* gene for expression from the X^P in the early embryo. Little is known about the maternal imprint. Although de novo DNA methylation is dispensable (28), *Xist*'s antisense partner, *Tsix*, plays a critical role in protecting the X^M from silencing (29–31), and the H3K9me3 mark correlates with *Xist* silencing (32).

The nature of the paternal germline imprint and the extent of its influence in the early embryo have been under some debate. In one school of thought, the paternal germ line marks the *Xist* gene for expression in the female embryo, but the mark is not read until later in preimplantation development (17). Another model suggests that X^P silencing mechanistically follows from meiotic sex chromosome inactivation in the male germ line (16, 33–37) and is a direct extension of the postmeiotic sex

Significance

Mammals with imprinted X inactivation demonstrate exclusive silencing of the paternal X chromosome. X-inactivation–specific transcript (Xist) RNA directs this silencing and is imprinted to be expressed only from the father's X chromosome. Here we investigate how *Xist* is imprinted. Using a transgenesis system, we find that *Xist* imprinting depends on its unpaired state in the father's germ line. When *Xist* is present in two copies (one each on homologous chromosomes) and therefore is paired during meiosis, the gene does not demonstrate paternal-specific expression in the female embryo. However, when *Xist* is present in only one copy and therefore lacks a pairing partner during meiosis, the gene shows strong imprinted expression. Thus, the unpaired state plays a critical role in epigenetic transmission between generations.

Author contributions: S.S. and J.T.L. designed research; S.S., B.P., S.N., J.Y.A., W.P., and J.C.-D. performed research; B.P. and H.S. contributed new reagents/analytic tools; S.S. and J.T.L. analyzed data; and S.S. and J.T.L. wrote the paper.

Reviewers: N.E., Temple University; and K.P., David Geffen School of Medicine at University of California, Los Angeles.

The authors declare no conflict of interest.

See Commentary on page 14408.

[1]Present address: Centre for Genomic Regulation, 08003 Barcelona, Spain.

[2]Present address: Center for Genome Engineering, Institute for Basic Science, Seoul 151-747, South Korea.

[3]To whom correspondence should be addressed. Email: lee@molbio.mgh.harvard.edu.

This article contains supporting information online at www.pnas.org/lookup/suppl/doi:10.1073/pnas.1519528112/-/DCSupplemental.

chromatin (22, 14). There is evidence that repetitive elements on the X^P are already silent at the time of zygotic gene activation in the two-cell embryo, with ensuing silencing of coding genes beginning at the four-cell stage (14).

Despite differences, the various models agree that Xist RNA is a crucial component of imprinted XCI. Previous work showed that various *Xic* transgenes (Tgs) can recapitulate chromosome-wide silencing on autosomes when introduced into embryonic stem cells and somatic cells (2, 9, 38). Given the ability of ectopic *Xist* Tgs to silence linked autosomal sequences, the observation that single-copy *Xist* YAC Tgs could be transmitted through the germ line without apparent consequences for development in the mouse embryo (39–41) might be somewhat unexpected; indeed, *Xist*-mediated silencing of linked autosomal genes would be expected to result in haploinsufficiency phenotypes if *Xist* were expressed. In these transgenesis experiments, YAC Tg53 and Tg80 lines bearing 210–460 kb of *Xic* sequences (Fig. 1*A*), including *Xist*, gave rise to paternal-only expression of *Xist* in preimplantation embryos, but both male and female embryos were viable and were born without distortion of the sex ratio or transmission (39, 41). Furthermore, adult transgenic animals were normal and fully fertile. These findings may suggest that the *Xist* YAC Tgs lost their influence during development and/or were not sufficient to establish long-range chromatin silencing fully in the first place. Thus, the necessary sequences for establishing and maintaining the *Xist* imprint remain an open question. As a first step toward answering the question, we ask how *Xist* becomes imprinted by the male germ line. Here we investigate mechanisms of *Xist* imprinting by creating transgenic lines carrying 200 kb of sequence from the *Xic* and by observing the consequences of Tg zygosity on *Xist* imprinting in the male germ line.

Results

Mice Carrying Autosomal *Xist* Transgenes Are Viable but Show Specific Phenotypes. To investigate the requirements for imprinting, we created transgenic mice by microinjecting the 200-kb BAC8 Tg carrying *Xist*, *Tsix*, and surrounding sequences (TgBAC8; Fig. 1*A*) into the pronuclei of fertilized mouse embryos. We obtained six independent Tg lines. In contrast to the lack of phenotype

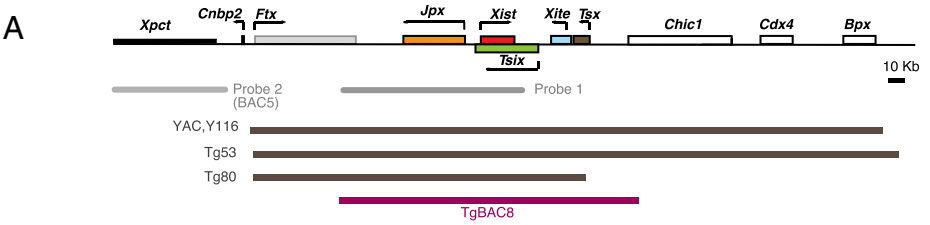

B

Tg line	Founder sex	Tg Integration	Tg copy number	Germline transmission	Phenotype
2080	♂	1	2 - 7	♂	Hemizygous female lethal
2082	♂	1	4 - 7	♂ & ♀	Homozygous lethal (both sexes)
2086	♀	1	2	♂ & ♀	Not found
2087	♀	1	2	♂ & ♀	Homozygous male sterile
2091	♀	1 (on X)	7 - 16	♀	Hemizygous male sterile
2092	♀	2	~ 30	♀	Hemizygous male sterile

C

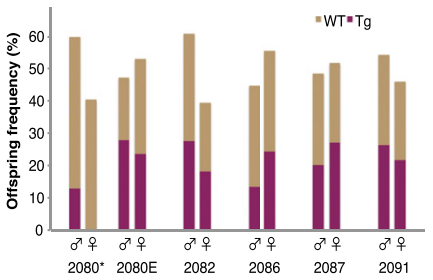

Line	Cross	Total N	Ave. litter size n	χ^2
2080*	+/+ ♀ X ♂Tg/+	77	4.5	$P < 0.01$ **
2080E	+/+ ♀ X ♂Tg/+	72	9.0	$P > 0.5$
2082	+/+ ♀ X ♂Tg/+	76	6.3	$P > 0.3$
2086	+/+ ♀ X ♂Tg/+ Tg/+ ♀ X ♂+/+	74	8.2	$P > 0.05$
2087	+/+ ♀ X ♂Tg/+ Tg/+ ♀ X ♂+/+	89	7.4	$P > 0.2$
2091	Tg/+ ♀ X ♂+/Y	174	6.7	$P > 0.4$

D

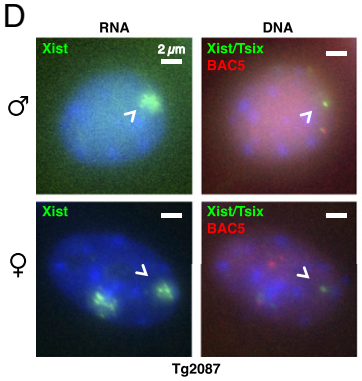

Tg Line		Fibro blasts Tg/+	Xist RNA cloud (%) Tg only	Xi	Xi + Tg	Total cells n
2080	♂		*53*	n.a.	n.a.	57 *
	♀		*0*	*52*	*48*	106 *
2082	♂		*62*	n.a.	n.a.	34
	♀		*0*	*42*	*58*	12
2086	♀		*0*	*69*	*31*	70
2087	♂		*75*	n.a.	n.a.	114
	♀		*0*	*41*	*59*	61
2091	♀		*0*	*23*	*77*	51
2092	♀		*0*	*56*	*44*	32

E

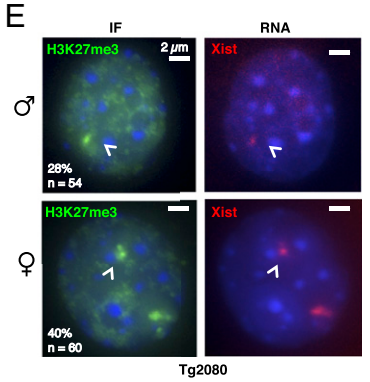

Fig. 1. Generation and characterization of *Xist* transgenic mice. (*A*) Map of *Xic*, FISH probes, YAC Tgs, and the BAC8 Tg. (*B*) Characteristics of the six BAC8 transgenic lines created in this study. (*C*) Absence of transmission ratio distortion of the Tg. (*Left*) Frequency of WT or transgenic (Tg/+) animals in the adult offspring. *Tg2080 was the only line did not produce any transgenic female adult, and the presence of embryonic offspring [pooled from embryonic day (E)3.5, E6.5, E12.5, and E18.5 embryos] was plotted (2080E). (*Right*) The genetic crosses that gave rise to the screened genotypes. Two-tailed χ^2 analysis, *P* compared with the expected ratio of WT/transgenic = 1; $^{**}P < 0.01$. (*D*) Xist activities on the Tg. (*Left*) Xist transcript coats the autosome *in cis*, as examined by RNA FISH in male and female tail fibroblasts isolated from Tg2087/+ pups; DNA FISH was performed with the BAC5 probe (probe 2 in *A*), which marks the endogenous *Xic*. Arrowheads indicate the Tg site as deduced by the absence of BAC5 DNA signal. (*Right*) Quantification of Xist RNA clouds in male and female tail fibroblasts isolated from six transgenic lines. Percentages are shown for cells expressing Xist from the transgenic or Xi chromosome or both. *Tg2080/+ did not produce viable adult offspring, and tail-tip fibroblasts were obtained from neonates. (*E*) The autosomal Tg recruits H3K27 trimethylation associated with the integration site, as examined by immunofluorescence (IF) combined with Xist RNA FISH in male and female embryonic fibroblasts isolated from Tg2080/+ animals. A focus of H3K27me3 associated with the Tg was observed in 28% of male cells ($n = 54$) and in 40% of female cells ($n = 60$). Arrowheads indicate Tg insertion sites.

observed previously with YAC Tgs (39–41), intriguing phenotypes were observed in five of the six hemizygous transgenic lines, here named Tg2080, Tg2082, Tg2086, Tg2087, Tg2091, and Tg2092 (Fig. 1*B*). Two of the lines, Tg2080 and Tg2092, were unstable and were lost after a few generations.

Tg2080/+ had a male founder that carried two to seven Tg copies at a single integration site. The male founder was fertile. Crossing to WT females, however, resulted in F1 progeny that showed a female-specific Tg lethality. Tg2080/+ females died during the neonatal period. On the other hand, Tg2080/+ males were found at reduced frequency. These viability differences were not observed in prenatal embryos, which were recovered at expected Mendelian frequencies regardless of sex (Fig. 1*C* and Fig. S1). Tg2082/+ also had a male founder that showed a single integration site with four to seven Tg copies. Although both male and female F1 hemizygotes were viable, homozygosity of the Tg resulted in zygotic lethality of both sexes. By contrast, Tg2086 had a female founder with a single integration site and a Tg copy number of 2. Tg2086/+ mice had no gross phenotype. Both female and male offspring produced litters of expected size and at normal Mendelian frequencies (Fig. 1*C*).

On the other hand, for several hemizygous Tg lines (Tg2087, Tg2091, and Tg2092), sterility was a major issue. Intriguingly, in each case, the sterility was observed only in the male. Notably, all three lines had female founders. In the case of Tg2087/+, male sterility occurred when the autosomal Tg was homozygosed. In the case of Tg2091/Y and Tg2092/+, male sterility was observed in the hemizygous state. Tg2091 is an X-linked integration with 7–16 copies of the Tg. Tg2092 had two integration sites for a total of 30 Tg copies.

To understand the basis of these phenotypes, we first examined *Xist* expression in somatic cells of the progeny. We isolated tail-tip fibroblasts from male and female progeny of each transgenic line and performed Xist RNA FISH with accompanying DNA FISH to distinguish the transgenic locus from the endogenous *Xic*. Robust expression of Xist RNA was observed from the hemizygous transgenic locus in both male and female cells from all transgenic lines (Fig. 1*D*). The Xist "cloud" produced by the Tg was qualitatively similar to the endogenous Xist cloud in the female cell. In the case of hemizygous Tg2087/+, for example, an Xist cloud was observed over the transgenic locus in 74.6% of male cells (n = 114). Among female cells, 59% showed two Xist clouds, one over the Xi and one over the autosomal insertion site;

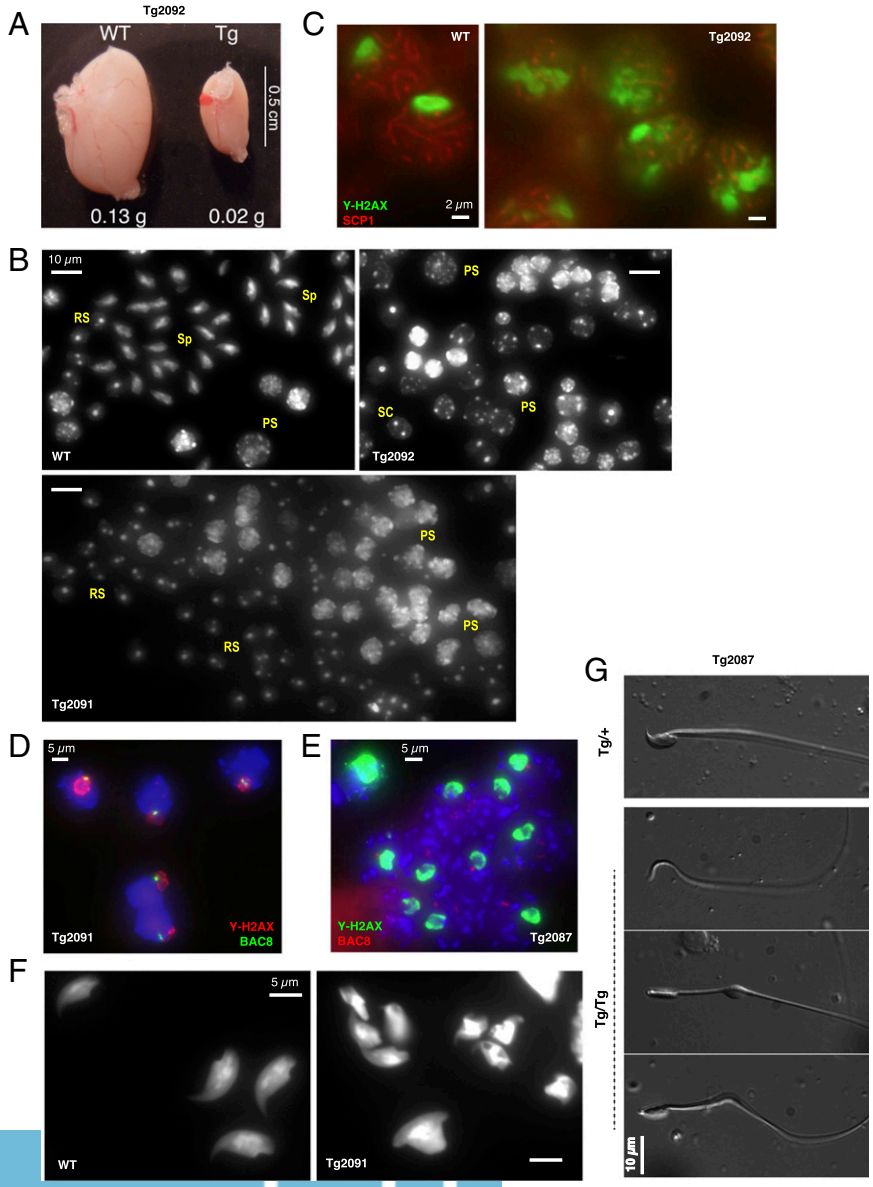

Fig. 2. Male germline defects in *Xist* transgenic mice. (*A*) Male hemizygous Tg2092 mice are sterile and have small testes. Shown are representative testes from a transgenic male and a WT littermate control male. (*B*) Pachytene arrest in the male germ line of hemizygous Tg2092 and Tg2091 mice. PS, pachytene spermatocytes. RS, round spermatids, SC, Sertoli cells; Sp, spermatozoa. (*C*) γH2AX and SCP1 immunostaining in pachytene spermatocytes reveal the XY body in WT mice and aberrant foci formation in Tg2092 mice. (*D*) Normal XY-body formation in the pachytene spermatocytes of hemizygous Tg2091 mice. Immunostaining fluorescence for γH2AX and DNA FISH for Tg BAC8 integration are shown. (*E*) Normal XY-body formation in the pachytene spermatocytes of homozygous (Tg/Tg) Tg2087 males. Immunostaining fluorescence for γH2AX and DNA FISH for Tg BAC8 are integration shown. (*F*) Defective spermatozoa of hemizygous Tg2091 male: Morphological abnormality in sperm heads of Tg2091 is visualized with DAPI in the spermatocytes spread. (*G*) Defective sperm cells of homozygous (Tg/Tg) Tg2087 males. Mature sperm isolated from epididymis of the homozygous Tg/Tg male (sterile) and the hemizygous +/Tg male (fertile). Sperm morphology was visualized by differential interference contrast.

41% showed an Xist cloud only over the Xi (n = 61). These experiments showed, somewhat surprisingly, that Xist remained robustly expressed in somatic cells well into adulthood despite potentially detrimental effects. Indeed, transgenic Xist was capable of recruiting PRC2 to trimethylate histone H3 at lysine 27 (H3K27me3) (Fig. 1*E*), consistent with formation of repressive chromatin.

Male-Specific Sterility and Germ-Cell Defects. Three of the six independent Tg/+ lines showed male-specific sterility. The Tg2092/+ line carried the highest number of Tg copies (~30), originally carried on two autosomes. Consistent with germ-cell defects, the testis mass of male mice was <20% that of WT littermates (Fig. 2*A*). Examination of male germ cells revealed that spermatogenesis was arrested at the pachytene stage of meiosis I (Fig. 2*B*). There were few, if any, germ cells of a more mature stage, including spermatozoa. Intriguingly, although pachytene spermatocytes of WT mice were characterized by a single large γ-H2AX domain localizing to the partially synapsed "sex body" or "XY body" (42), Tg2092 spermatocytes showed multiple γ-H2AX domains beyond the XY body (Fig. 2*C*). Such aberrant γ-H2AX distributions were prevalent and were observed in 78% (n = 50) of pachytene meiotic cells from Tg2092/+ males. Because γ-H2AX is induced by meiotic asynapsis and is associated with meiotic silencing by unpaired chromatin (43), the occurrence of multiple diffuse γ-H2AX domains suggested multiple aberrant synapses and chromatin changes in the presence of the *Xist* Tg.

Although the multiple γ-H2AX domains were consistent with there being multiple Tg integration sites, the size of the domains indicated that γ-H2AX must have spread along the autosomes beyond the several hundred kilobases or several megabases associated with the tandem Tgs. These autosomal abnormalities likely accounted for the sterility of Tg2092 males. The Tg2092 genotype therefore could be transmitted only maternally. Unfortunately, because the Tgs were inserted into two distinct autosomes, the Tgs were unstable and also segregated after one generation of passage, and the original Tg2092 genotype could not be maintained for further analysis.

The hemizygous Tg2091 and homozygous Tg2087 male mice were sterile also, despite having normal γ-H2AX localization on the XY body (Fig. 2 *D* and *E*). On the XY body, a defined γ-H2AX domain was present in 76% (n = 51) of 2091 Tg/Y pachytene spermatocytes and in 69% (n = 96) of 2087 Tg/Tg pachytene spermatocytes. The presence of microγ-H2AX signals on the unpaired Tgs could not be ruled out, because small regions of H2AX phosphorylation could be present at domains of

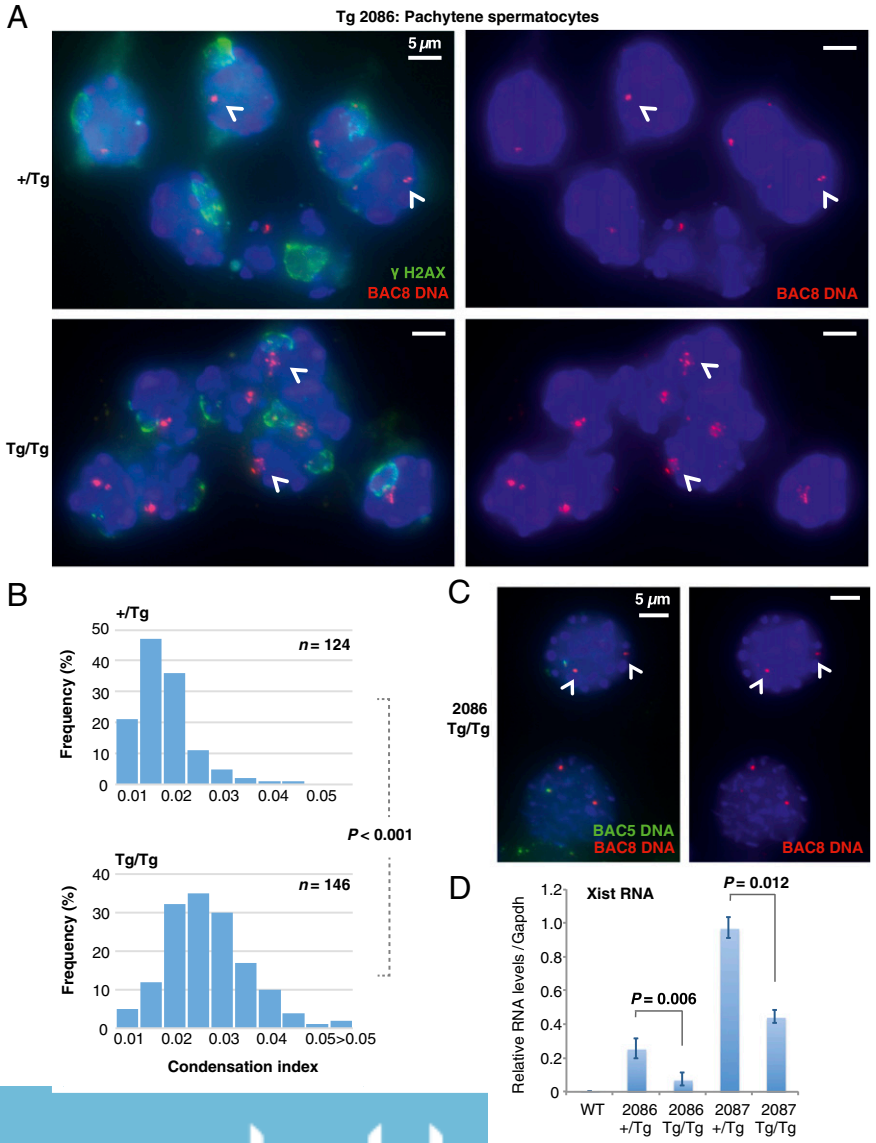

Fig. 3. Epigenetic consequences of the +/Tg versus Tg/Tg states in the male germ line. (*A*) Pachytene spermatocytes from Tg2086 males. Hemizygous (+/Tg) or homozygous (Tg/Tg) transgenic integrations examined by immunostaining/DNA FISH and DAPI. The pachytene stage is identified by the presence of the XY body γH2AX domain. On the XY body, a defined γ-H2AX domain was present in 64% (n = 139) of +/Tg pachytene spermatocytes and in 63% (n = 116) of Tg/Tg pachytene spermatocytes. DNA FISH was carried out using a BAC8 DNA probe, which marks the transgenic *Xist* outside the XY body γH2AX domain. Arrowheads indicate Tg insertion sites. (*B*) Quantitation of chromatin decompaction. Z-stack images were captured at 0.2-μm intervals using a Zeiss LSM780 confocal microscope, and the 3D image was projected on a single 2D plane. Using image analysis tools in the Volocity software, we measured the size and spread of the DNA FISH signal by drawing a minimal loop that is inclusive of the full signal. The area within the loop represents the Tg chromatin spread (a). We measured the nucleus size (A) by drawing a loop covering the full DAPI signal. The spread of the DNA FISH signal (a) divided by the size of the corresponding nucleus (A) is the normalized compass (N.C.). N.C. = a/A, which is the condensation index. n, number of cells measured for each genotype. P, statistical significance of difference between the two distribution profiles (+/Tg versus Tg/Tg) calculated by the nonparametric Kolmogorov–Smirnov test. (*C*) DNA FISH of spermatogonial cells from 2086 Tg/Tg males. The BAC5 DNA probe (probe 2 in Fig. 1*A*) marks the endogenous *Xic*; the BAC8 DNA probe marks the transgenic *Xist*. Arrowheads indicate Tg insertion sites. (*D*) *Xist* expression levels in the testes. qRT-PCR of *Xist* normalized by *Gapdh* for WT and transgenic testis samples. +/Tg and Tg/Tg males are littermates obtained from the Tg2086 or Tg2087 mouse line. Triplicates were performed for each sample. Averages ± SE are shown. The P values indicated in the pairwise comparisons were determined by the one-tail t test.

several hundred kilobases without being detectable at the level of immunostaining. This asynapsis and any resulting recruitment of the double-strand break repair mechanism could lead to localized silencing (43, 44). Interestingly, 2091 Tg/Y and 2087 Tg/Tg males showed morphological anomalies in the spermatozoa. In the case of Tg2091, dysmorphic head shapes and failed separation of meiotic tetrads were readily apparent (Fig. 2*F*). There was an absence of mature spermatozoa in the epididymis. In the case of Tg2087, the homozygous males carried mature sperm in the epididymis but failed to sire offspring. Examination of mature spermatozoa revealed heterogeneous morphological abnormalities ranging from a kinked tail to a missing head (Fig. 2*G*). These anomalies were present only in the homozygous state and provided logical explanations for the male-specific sterility. The female counterparts were fully fertile.

Xist Imprinting: Epigenetic Effects of Transgene Hemizygosity. Unlike the high-copy-number Tg2092/+ line, transgenic lines with low-copy *Xist* integrations generally showed normal XY bodies in pachytene spermatocytes (Figs. 2 *D* and *E* and 3*A*). In the male germ line, large regions of asynapsed chromatin are known to be subject to meiotic silencing, as observed in cases of chromosomal translocations (43, 45), and can interfere with meiotic sex chromosome inactivation (46). Our *Xic* Tg was 200 kb, and its insertion at low copy numbers (two to seven times) did not obviously interfere with the meiotic synapsis. Intriguingly, however, the ectopic *Xic* chromatin was changed by the unpaired state of the Tg, most evidently during the pachytene stage of meiosis (Fig. 3*A*). DNA FISH using BAC8 as a probe showed the ectopic *Xic*, when hemizygous (+/Tg) in the male germ line, to be compact chromatin visualized as a small and tight pinpoint signal (Tg2086 is shown as an example in Fig. 3*A*). This compact signal is typical of observations of BAC8 Tgs in somatic cells (e.g., in mouse embryonic fibroblasts) (Fig. 1*D*) and therefore was not surprising.

On the other hand, when present in the homozygous stage (Tg/Tg), the *Xic* chromatin became decompacted, with the DNA FISH signals appearing much more diffuse than typical for somatic cells (Fig. 3*A*, *Lower*). To quantitate this difference, we performed DNA FISH and compared the sizes of the BAC8 transgenic signals in Tg/Tg versus +/Tg cells (Fig. 3*B*). We captured z-stack images at 0.2-μm intervals and measured the size and spread of the DNA FISH signals, expressed in terms of a "condensation index," as defined by the normalized compass (see the legend of Fig. 3*B*). A significant difference was observed between the sizes of the Tg loci in +/Tg versus Tg/Tg cells, with loci in Tg/Tg cells occupying a greater territory and, hence, being more open (Fig. 3*B*). On the other hand, when the 2086 Tg/Tg spermatocytes had not yet entered meiosis (spermatogonial cells), the BAC8 transgenic loci were well separated, and both loci appeared as small pinpoints (Fig. 3*C*). We conclude that pachytene chromatin is treated differently during pachytene and that the hemizygous, unpaired state of BAC8 sequences resulted in a greater degree of chromatin compaction.

The compaction state of chromatin has been well correlated with the gene activity state, with condensed chromatin associated with gene repression and decondensed chromatin associated with gene activation (47–49). Therefore one might predict that the Tg would be better expressed in the more open chromatin of the homozygous state. However, we were surprised to see increased *Xist* expression in the +/Tg state and lower expression in the Tg/Tg state (Fig. 3*D*; elevated Xist expression of the +/Tg cells was not associated with a large Xist cloud). This paradoxical finding is consistent with a previous report indicating that *Xist* expression is favored by the heterochromatic state of the *Xic* in somatic cells (50) and also is consistent with *Xist* being expressed only from the silent Xi (8). Thus, hemizygosity affects not only the chromatin compaction of the Tg but also its expression status during male pachytene. We conclude that *Xist* expression is favored, in general, by condensed chromatin.

Paternal Effects: Xist Imprinting Promoted by Hemizygosity. The effect of the hemizygous state on Xist expression was arguably small (twofold). However, because *Xist* normally is expressed only at very low levels in the male germ line (several RNA copies

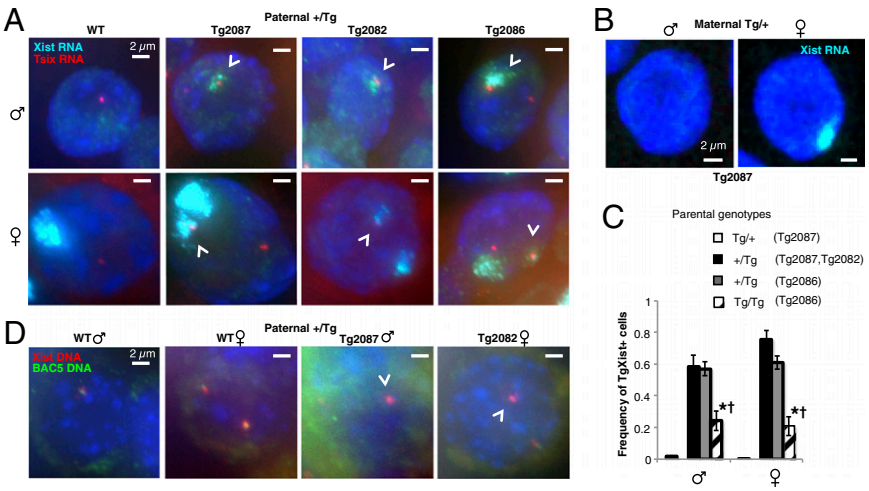

Fig. 4. Imprinted Xist expression in the transgenic preimplantation embryo. (*A*) Transgenic *Xist* expression was observed in trophectoderm cells of blastocyst-stage (E3.5) embryos in which the Tg was inherited exclusively from the father (+/Tg) by crossing heterozygous fathers to WT mothers. Xist and Tsix RNA FISH were performed using strand- and locus-specific LNA or DNA oligonucleotide probes. Trophectodermal cells were sampled from the mural trophectoderm surrounding the blastocoel to avoid inner cell mass cells located at the polar region of the embryo. Arrowheads indicate Tg insertion sites. (*B*) No transgenic *Xist* expression was detected in trophectoderm cells of blastocyst-stage (E3.5) embryos when the Tg was inherited exclusively from the mother (Tg/+) by crossing heterozygous mothers to WT fathers. Xist RNA FISH was performed using locus-specific LNA probes. (*C*) Transgenic Xist expression in the blastocyst was affected by the Tg zygosity of the father but not of the mother. For each transgenic embryo (E3.5 blastocyst) with Tg derived from the father, the percentage of cells showing transgenic *Xist* expression was counted. At least five embryos were analyzed for each category. †TgXist RNAs in Tg/Tg cells were qualitatively different, ranging from small pinpoints to modest RNA clouds (Fig. 5). Averages ± SE are shown. *$P < 0.05$ as calculated by Student's *t* test comparing the result of Tg/Tg father with that of +/Tg fathers, both from Tg2086. By convention, the maternal genotype is noted first: Tg/+, maternal transmission; +/Tg, paternal transmission. (*D*) Xist and BAC5 DNA FISH was performed after the RNA FISH of cells shown in *A*, with the BAC5 probe (probe 2 in Fig. 1*A*) marking the endogenous *Xic*. The Tg (arrowheads) is indicated by Xist DNA signal (red) that is not associated with the BAC5 DNA signal (green).

only) (18, 19), the small decrease was likely all that could be observed in the germ line. *Xist* is not fully up-regulated until the gene is passed on to female progeny. In mice, the paternal *Xist* allele is induced initially in the two-cell embryo and becomes fully up-regulated in the morula (14, 16, 17, 22, 41). This paternal-specific *Xist* expression is responsible, at least in part, for imprinted XCI in the early mouse embryo and in extraembryonic tissues of later-stage embryos (5, 7, 16, 41).

To determine whether the hemi- or homozygosity of the Tg could affect its imprinting, we tested transgenic *Xist* expression in blastocysts resulting from Tg/Tg versus +/Tg fathers using the Tg2086 line, the only line without the sterility or lethality phenotypes that would preclude homozygosis. In agreement with previous reports on up-regulation of the paternal *Xist* in the zygotes (41, 51), transgenic *Xist* inherited from a hemizygous Tg father showed significant expression in the trophectoderm, an early extraembryonic tissue first formed in the blastocyst (Fig. 4*A*). On the other hand, transmission from a hemizygous mother did not result in *Xist* expression in either male or female embryos (Tg/+; Fig. 4 *B* and *C*). Thus, the effect of hemizygosity on imprinting is paternal specific, as is consistent with an activating *Xist* imprint being applicable only in the male germ line [repressive imprinting being a maternal-specific phenomenon (24–26)]. The paternal-only Tg expression was observed in both sons and daughters of the +/Tg father, indicating a true imprinting phenotype rather than a sex-specific property and arguing that the paternal germline imprints the *Xist* gene irrespective of the sex of the inheriting progeny. By performing DNA FISH using a combination of a *Xist* probe and a nonoverlapping *Xic* probe (BAC5, outside the BAC8 sequence; probe 2 in Fig. 1*A*), we could distinguish between the transgenic and the endogenous loci (Fig. 4*D*). The endogenous *Xist* gene was silent in all cells of the male embryo, but it was up-regulated in one of two female X chromosomes in the female embryo, as expected (Fig. 5 *A* and *B*). These observations held true for multiple independent transgenic lines (e.g., Tg2087, Tg2082, and Tg2086) (Fig. 4*A*). We therefore conclude that the BAC8 Tg carries sufficient genetic information to imprint *Xist* correctly.

A previous study suggested that *Xist* imprinting was not affected by the hemi- or homozygosity of the *Xist* Tg in the male germ line (41). However, as discussed above, the Tg53/Tg80 Tgs may not be fully sufficient to recapitulate imprinted XCI. Given the effects of zygosity on chromatin decompaction and pachytene expression in our transgenic system (Fig. 3), we asked whether imprinting also might be affected by homozygosity of the Tg. Most intriguingly, homozygosing the Tg in the paternal germ line significantly reduced transgenic Xist expression in the trophectoderm (Figs. 4*C* and 5 *A* and *B*). In resulting transgenic male embryos, the number of Xist-expressing cells was reduced

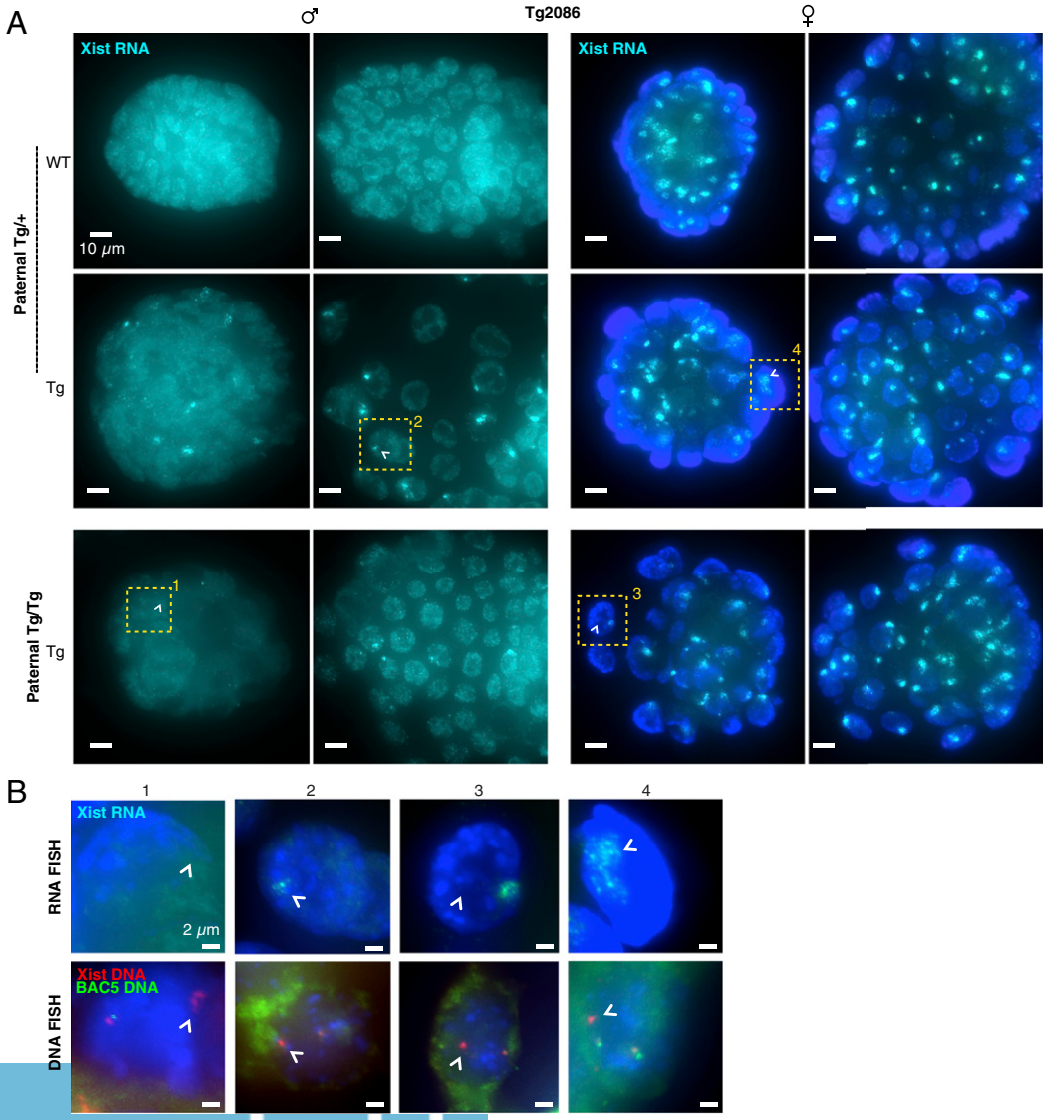

Fig. 5. Imprinted Xist expression in the progeny is promoted by a hemizygous state in the paternal germ line. (*A*) Representative E3.5 blastocysts with Xist RNA FISH (Cy5, light blue) and DAPI. Two embryos are shown for each genotype. WT and transgenic embryos derived from heterozygous +/Tg fathers crossed with WT mothers (*Top* and *Middle*) and transgenic embryos derived from homozygous Tg/Tg fathers crossed with WT mothers (*Bottom*). Male and female embryos from Tg2086 are shown. Boxed nuclei in *A* are magnified in *B*. Arrowheads Indicate transgenic locus. (*B*) Xist RNA FISH followed by Xist and BAC5 DNA FISH of the nuclei boxed in *A*. Arrowheads depict the transgenic *Xist* locus. The endogenous versus transgenic *Xist* locus is distinguished by hybridization to the BAC5 probe, which detects only the endogenous locus.

dramatically in the embryos inheriting the Tgs from a homozygous father, and Xist was absent in most of the cells (example 1 in Fig. 5*B*). In resulting female embryos, the number of trophectodermal cells with two Xist RNA clouds (one transgenic, one endogenous) was reduced similarly, and the transgenic Xist cloud was mostly absent (example 3 in Fig. 5*B*). Additionally, among the minority of Tg/Tg cells that did express transgenic Xist, the Xist foci ranged from small pinpoints to modest RNA clouds and therefore were qualitatively different from normal Xist clouds (Fig. 5). Thus, although the Tg carries sufficient genetic information to imprint *Xist*, imprinting cannot be executed properly when the Tg is present in the homozygous state during male meiosis.

Discussion

Both the maternal and paternal germ lines play critical roles in imprinting the X chromosome for dosage compensation (24–27, 29, 32). Although the maternal germ line lays down a repressive mark that precludes *Xist* expression from the X^M in the early embryo, the paternal germ line imprints a permissive mark that drives *Xist* expression from the X^P (Fig. 6*A*). Our present work has elucidated one aspect of how the imprint is applied to *Xist* on the X^P. The work demonstrates that (*i*) the information necessary for paternal *Xist* imprinting is contained with the 200-kb BAC8 Tg and (*ii*) the cross-generational imprinting effect results directly from the unpartnered or hemizygous state of the *Xist* locus in the male germ line.

In our transgenic model (Fig. 6*B*), the 200-kb BAC8 Tg includes essential noncoding regulatory elements flanking *Xist* and is sufficient for ectopic *Xist* expression and long-range chromatin silencing *in cis*. The unpartnered *Xist* Tgs account for several hundred kilobases to several megabases of nonhomologous DNA sequence on autosomes (Fig. 1*B*) and are chromatinized in a manner similar to the XY body (Fig. 2). The phenomenon we observe is likely related to the extent of nonhomology rather than to Tg copy number per se. Higher copy numbers of the Tg would promote extensive hemizygosity and, in our study, are correlated with phenotypic defects affecting viability and/or fertility. Judging by the highly visible accumulation of γ-H2AX at Tg sites in many lines (Fig. 2), we infer a behavior analogous to the meiotic sex chromosomes and propose that the hemizygous—and therefore unpartnered or unpaired—state of *Xist* in the male germ line partly drives the imprinting of this gene. One attractive mechanism might involve meiotic silencing by unpaired DNA (MSUD) or chromatin (37, 52), a genome-defense phenomenon first described in fungi meiosis where the absence of pairing or synapsis triggers a silencing mechanism limited to the unpaired chromatin segment (52). The phenomenon also occurs in mammals (37).

We postulate that chromatin modifications resulting from the unpaired state of the X-inactivation center may be directly responsible for imprinting *Xist* and account for the paternal-specific *Xist* expression in the next generation. Thus, *Xist* imprinting appears to depend on both (*i*) sequences specific to the *Xic* contained within the 200-kb BAC8 Tg that would render *Xist* receptive to imprinting, and (*ii*) passage of those sequences through the male germ line as a nonhomologous, unpaired chromosomal region to mark the *Xist* gene (Fig. 6). At the same time, the unpaired state of the X chromosome may result in imprinting of the X-linked repetitive elements (14). Together, the imprinting of *Xist* and repetitive elements may partially underlie imprinted XCI. In mice, genomic imprinting of autosomal loci occurs prenatally in prospermatogonia (53) and without obvious involvement of meiotic asynapsis. Thus, different mechanisms may be used by imprinted XCI and autosomal imprinting.

Materials and Methods

Generation of Transgenic Mice. Purified BAC8 DNA (clone 399K20) (54) was microinjected pronuclearly into fertilized embryos, which were transplanted into recipients for the creation of transgenic mice. Microinjection and the production of transgenic animals were carried out by the Transgenic and Gene Targeting Facility (Massachusetts General Hospital). The presence and copy number of BAC8 was assessed by PCR and quantitative PCR (qPCR) on tail or toe DNA using primers against the BAC8 vector sequence as well as five unique genomic regions in the 194.4-kb BAC8 insert sequence. *Hprt* and *Pgk* genomic primers were used for internal controls. Primers used were pB4 forward: AGTTGGAACCTCTTACGTGCCGAT and reverse: ATGTGGTGTGACCGGAACAGAGAA; Sp85 forward: GGGTCTCTACCTATCAACAAATAGAATC and reverse: TTACTGAAGGAACTTTAGACAGGAATGTAG; Xist_E1 forward: CGGTTCTTCCGTGGTTTCTC and reverse: GGTAAGTCCACCATACACAC; BAC8_3 forward: GGTTTAGGCTCCATTCTTAAGACCTCAT and reverse: GGTCTACAGAGCTAGTTCCAAGACACCA; BAC8_4 forward: ATCCAGGACACCAGGATTCTCC and reverse: CATCTAGAAACACTAGCTTGAGAGG; BAC8_5 forward: TTCAATTGTTTAATGAAATATCCACA and reverse: GGGGTATCATAAAGGTGCTG; Hprt forward: CTGCTACTTCAACTCCTGGTGTGC and reverse: AGGCGAATTGGGATGTAGCTCAG; and Pgk1 forward: AAGGGCTCAGATTCTCAGGACTC and reverse: GTTTCGGATTCGTCACGGATGGTC. Transgene integration was verified by DNA FISH on fibroblasts isolated from skin or tail. Mouse experiments were conducted under oversight of the Institutional Animal Care and Use Committees (IACUC) at Massachusetts General Hospital and University of California, Irvine.

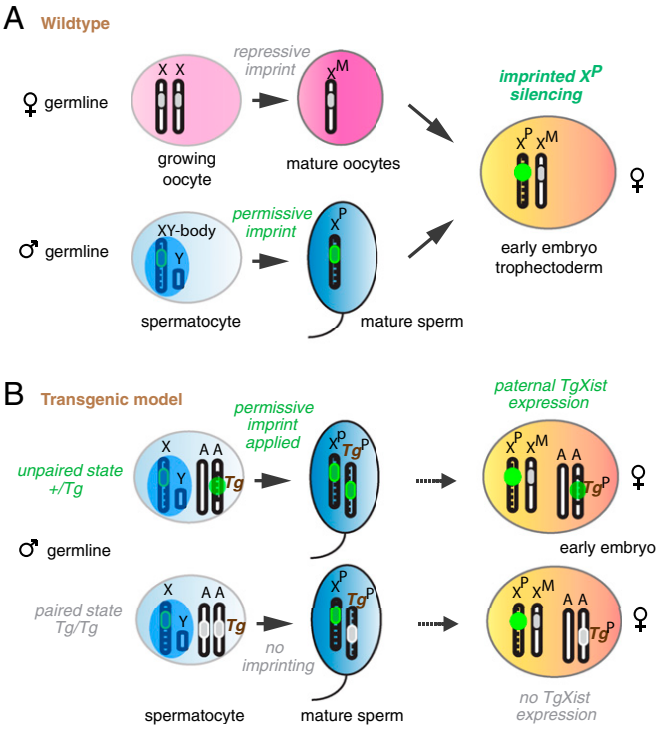

Fig. 6. *Xist* imprinting is promoted by the hemizygous state in the paternal germ line. (*A*) In the WT germ line, imprints are applied to both the X^M and the X^P. The X^M imprint (gray) is repressive for *Xist* expression in the early embryo, whereas the X^P imprint (green) is permissive for *Xist* expression. In the XY body, *Xist* lacks a pairing partner, and the unpaired state promotes its imprinting. (*B*) In the transgenic animal, imprinting of *Xist* is promoted by the hemizygous state (green) of the Tg in the male germ line, and Tg*Xist* is expressed in the early embryo. When the Tg is homozygosed (paired; gray), *Xist* expression is repressed in the early embryo.

RNA FISH, DNA FISH, and Immunostaining. FISH and immunostaining in cells were performed as described in refs. 55 and 56. FISH and immunostaining in meiotic spermatocytes and embryos followed the published protocol (57). For immunofluorescence, cells were blocked with PBS, 0.2% Tween20, 1% BSA. Anti-H3K27me3 (no. 39535; Active Motif) (1:100), anti-γH2AX (JBW301; Upstate) (1:5,000), or anti-SCP1 biotin (Novus Biologicals) (1:300) were incubated at room temperature for 1–2 h, followed by three washings of 5 min each in PBS and 0.2% Tween20, were incubated with secondary antibodies at 1:500 for 1 h at room temperature followed by three more washings, and were mounted in VECTASHIELD with DAPI (Vector Laboratories). For Xist RNA-FISH, a fluorescein-12-dUTP–labeled DNA probe or Cy5-labeled locked nucleic acid (LNA) was used. Tsix RNA-FISH was performed using Cy3-labled ssDNA oligo probes. For DNA FISH combined with RNA FISH

immunostaining, RNA FISH or immunostaining was performed first. Slides were postfixed in 4% (wt/vol) paraformaldehyde, treated with RNase A, and denatured. Images were collected using Nikon Eclipse 90i and Zeiss LSM780 microscopes and were analyzed with Volocity software (PerkinElmer).

Quantitative Measurement of the Chromatin Domain. Z-section images were captured with the Zeiss LSM780 confocal system. Image analysis and measurements were performed using Volocity software on projected 2D planes generated from stacked z-sections. The normalized compass is defined as *a*/*A*, where *a* measures the area of Tg chromatin spread by DNA FISH and *A* measures the corresponding nucleus size by DAPI.

qRT-PCR. Total RNA was isolated using TRIzol (Life Technology) and treated with TURBO DNase (Life Technology). One microgram of RNA was reverse-transcribed using the SuperScript III first-strand reverse transcription kit (Life Technology). qPCR was performed using VeriQuest SYBR qPCR Master Mix (Affymetrix) on the Chromo 4 DNA engine (Bio-Rad). Ct values were normalized to *Gapdh* to calculate the relative expression levels. Primer pairs were as follows: Xist NS33, CAGAGTAGCGAGGACTTGAAGAG; NS66, GCTGGTTCGTCTATCTTGTGGG (58); *Gapdh* forward, ATGAATACGGCTACAGCAACAGG; *Gapdh* reverse, GAGATGCTCAGTGTTGGGGG (38).

ACKNOWLEDGMENTS. We thank members of the Lee laboratory for valuable discussions and suggestions, the University of California, Irvine (UCI) Optical Biology Core Facility for use of the Zeiss LSM780 system, and the UCI Transgenic Mouse Facility for assistance with mouse embryos. This work was funded by NIH Grant R01-GM58839 (to J.T.L.) and by start-up funds from UCI (to S.S.). J.T.L. is an Investigator of the Howard Hughes Medical Institute.

1. Lyon MF (1961) Gene action in the X-chromosome of the mouse (Mus musculus L.). *Nature* 190:372–373.
2. Wutz A, Gribnau J (2007) X inactivation Xplained. *Curr Opin Genet Dev* 17(5):387–393.
3. Payer B, Lee JT (2008) X chromosome dosage compensation: How mammals keep the balance. *Annu Rev Genet* 42:733–772.
4. Starmer J, Magnuson T (2009) A new model for random X chromosome inactivation. *Development* 136(1):1–10.
5. Takagi N, Sasaki M (1975) Preferential inactivation of the paternally derived X chromosome in the extraembryonic membranes of the mouse. *Nature* 256(5519):640–642.
6. Graves JAM (1996) Mammals that break the rules: Genetics of marsupials and monotremes. *Annu Rev Genet* 30:233–260.
7. Payer B, Lee JT, Namekawa SH (2011) X-inactivation and X-reactivation: Epigenetic hallmarks of mammalian reproduction and pluripotent stem cells. *Hum Genet* 130(2): 265–280.
8. Brown CJ, et al. (1991) A gene from the region of the human X inactivation centre is expressed exclusively from the inactive X chromosome. *Nature* 349(6304):38–44.
9. Lee JT, Strauss WM, Dausman JA, Jaenisch R (1996) A 450 kb transgene displays properties of the mammalian X-inactivation center. *Cell* 86(1):83–94.
10. Brown CJ, et al. (1992) The human XIST gene: Analysis of a 17 kb inactive X-specific RNA that contains conserved repeats and is highly localized within the nucleus. *Cell* 71(3):527–542.
11. Penny GD, Kay GF, Sheardown SA, Rastan S, Brockdorff N (1996) Requirement for Xist in X chromosome inactivation. *Nature* 379(6561):131–137.
12. Marahrens Y, Panning B, Dausman J, Strauss W, Jaenisch R (1997) Xist-deficient mice are defective in dosage compensation but not spermatogenesis. *Genes Dev* 11(2): 156–166.
13. Kalantry S, Purushothaman S, Bowen RB, Starmer J, Magnuson T (2009) Evidence of Xist RNA-independent initiation of mouse imprinted X-chromosome inactivation. *Nature* 460(7255):647–651.
14. Namekawa SH, Payer B, Huynh KD, Jaenisch R, Lee JT (2010) Two-step imprinted X inactivation: Repeat versus genic silencing in the mouse. *Mol Cell Biol* 30(13): 3187–3205.
15. Lee JT, Davidow LS, Warshawsky D (1999) Tsix, a gene antisense to Xist at the X-inactivation centre. *Nat Genet* 21(4):400–404.
16. Huynh KD, Lee JT (2003) Inheritance of a pre-inactivated paternal X chromosome in early mouse embryos. *Nature* 426(6968):857–862.
17. Okamoto I, Otte AP, Allis CD, Reinberg D, Heard E (2004) Epigenetic dynamics of imprinted X inactivation during early mouse development. *Science* 303(5658): 644–649.
18. Salido EC, Yen PH, Mohandas TK, Shapiro LJ (1992) Expression of the X-inactivation-associated gene XIST during spermatogenesis. *Nat Genet* 2(3):196–199.
19. Ayoub N, Richler C, Wahrman J (1997) Xist RNA is associated with the transcriptionally inactive XY body in mammalian male meiosis. *Chromosoma* 106(1):1–10.
20. McCarrey JR, et al. (2002) X-chromosome inactivation during spermatogenesis is regulated by an Xist/Tsix-independent mechanism in the mouse. *Genesis* 34(4): 257–266.
21. Heard E, Disteche CM (2006) Dosage compensation in mammals: Fine-tuning the expression of the X chromosome. *Genes Dev* 20(14):1848–1867.
22. Namekawa SH, et al. (2006) Postmeiotic sex chromatin in the male germline of mice. *Curr Biol* 16(7):660–667.
23. Lee JT (2012) Epigenetic regulation by long noncoding RNAs. *Science* 338(6113): 1435–1439.
24. Kay GF, Barton SC, Surani MA, Rastan S (1994) Imprinting and X chromosome counting mechanisms determine Xist expression in early mouse development. *Cell* 77(5):639–650.
25. Goto Y, Takagi N (2000) Maternally inherited X chromosome is not inactivated in mouse blastocysts due to parental imprinting. *Chromosome Res* 8(2):101–109.
26. Tada T, et al. (2000) Imprint switching for non-random X-chromosome inactivation during mouse oocyte growth. *Development* 127(14):3101–3105.
27. Oikawa M, et al. (2014) Understanding the X chromosome inactivation cycle in mice: A comprehensive view provided by nuclear transfer. *Epigenetics* 9(2):204–211.
28. Chiba H, et al. (2008) De novo DNA methylation independent establishment of maternal imprint on X chromosome in mouse oocytes. *Genesis* 46(12):768–774.
29. Lee JT (2000) Disruption of imprinted X inactivation by parent-of-origin effects at Tsix. *Cell* 103(1):17–27.
30. Ohhata T, Hoki Y, Sasaki H, Sado T (2006) Tsix-deficient X chromosome does not undergo inactivation in the embryonic lineage in males: Implications for Tsix-independent silencing of Xist. *Cytogenet Genome Res* 113(1-4):345–349.
31. Maclary E, et al. (2014) Differentiation-dependent requirement of Tsix long non-coding RNA in imprinted X-chromosome inactivation. *Nat Commun* 5:4209.
32. Fukuda A, et al. (2014) The role of maternal-specific H3K9me3 modification in establishing imprinted X-chromosome inactivation and embryogenesis in mice. *Nat Commun* 5:5464.
33. Cooper DW (1971) Directed genetic change model for X chromosome inactivation in eutherian mammals. *Nature* 230(5292):292–294.
34. Lyon MF (1999) Imprinting and X chromosome inactivation. *Results and problems in cell differentiation*, ed Ohlsson R (Springer, Heidelberg), pp 73–90.
35. McCarrey JR (2001) *X-Chromosome Inactivation During Spermatogenesis: The Original Dosage Compensation Mechanism in Mammals? Gene Families: Studies of DNA, RNA, Enzymes, and Proteins*, eds Xue G, et al. (World Scientific, Teaneck, NJ), pp 59–72.
36. Greaves IK, Rangasamy D, Devoy M, Marshall Graves JA, Tremethick DJ (2006) The X and Y chromosomes assemble into H2A.Z-containing facultative heterochromatin following meiosis. *Mol Cell Biol* 26(14):5394–5405.
37. Turner JM, Mahadevaiah SK, Ellis PJ, Mitchell MJ, Burgoyne PS (2006) Pachytene asynapsis drives meiotic sex chromosome inactivation and leads to substantial post-meiotic repression in spermatids. *Dev Cell* 10(4):521–529.
38. Jeon Y, Lee JT (2011) YY1 tethers Xist RNA to the inactive X nucleation center. *Cell* 146(1):119–133.
39. Heard E, et al. (1996) Transgenic mice carrying an Xist-containing YAC. *Hum Mol Genet* 5(4):441–450.
40. Matsuura S, Episkopou V, Hamvas R, Brown SDM (1996) Xist expression from an Xist YAC transgene carried on the mouse Y chromosome. *Hum Mol Genet* 5(4):451–459.
41. Okamoto I, et al. (2005) Evidence for de novo imprinted X-chromosome inactivation independent of meiotic inactivation in mice. *Nature* 438(7066):369–373.
42. Turner JM (2007) Meiotic sex chromosome inactivation. *Development* 134(10): 1823–1831.
43. Turner JM, et al. (2005) Silencing of unsynapsed meiotic chromosomes in the mouse. *Nat Genet* 37(1):41–47.
44. Carofiglio F, et al. (2013) SPO11-independent DNA repair foci and their role in meiotic silencing. *PLoS Genet* 9(6):e1003538.
45. Baarends WM, et al. (2005) Silencing of unpaired chromatin and histone H2A ubiquitination in mammalian meiosis. *Mol Cell Biol* 25(3):1041–1053.
46. Homolka D, Ivanek R, Capkova J, Jansa P, Forejt J (2007) Chromosomal rearrangement interferes with meiotic X chromosome inactivation. *Genome Res* 17(10):1431–1437.
47. Müller WG, Walker D, Hager GL, McNally JG (2001) Large-scale chromatin decondensation and recondensation regulated by transcription from a natural promoter. *J Cell Biol* 154(1):33–48.
48. Eskeland R, et al. (2010) Ring1B compacts chromatin structure and represses gene expression independent of histone ubiquitination. *Mol Cell* 38(3):452–464.
49. Bickmore WA, van Steensel B (2013) Genome architecture: Domain organization of interphase chromosomes. *Cell* 152(6):1270–1284.
50. Sun BK, Deaton AM, Lee JT (2006) A transient heterochromatic state in Xist preempts X inactivation choice without RNA stabilization. *Mol Cell* 21(5):617–628.
51. Grant SG, Chapman VM (1988) Mechanisms of X-chromosome regulation. *Annu Rev Genet* 22:199–233.
52. Shiu PK, Raju NB, Zickler D, Metzenberg RL (2001) Meiotic silencing by unpaired DNA. *Cell* 107(7):905–916.
53. Barlow DP, Bartolomei MS (2014) Genomic imprinting in mammals. *Cold Spring Harb Perspect Biol* 6(2):a018382.
54. Augui S, et al. (2007) Sensing X chromosome pairs before X inactivation via a novel X-pairing region of the Xic. *Science* 318(5856):1632–1636.
55. Lee JT, Lu N (1999) Targeted mutagenesis of Tsix leads to nonrandom X inactivation. *Cell* 99(1):47–57.
56. Zhang LF, Huynh KD, Lee JT (2007) Perinucleolar targeting of the inactive X during S phase: Evidence for a role in the maintenance of silencing. *Cell* 129(4):693–706.
57. Namekawa SH, Lee JT (2011) Detection of nascent RNA, single-copy DNA and protein localization by immunoFISH in mouse germ cells and preimplantation embryos. *Nat Protoc* 6(3):270–284.
58. Stavropoulos N, Lu N, Lee JT (2001) A functional role for Tsix transcription in blocking Xist RNA accumulation but not in X-chromosome choice. *Proc Natl Acad Sci USA* 98(18):10232–10237.